EFFECTIVE THERMAL CONDUCTIVITY OF METAL HYDRIDE POWDERS: MEASUREMENT AND THEORETICAL MODELLING

J. Kallweit and E. Hahne

Institut für Thermodynamik und Wärmetechnik, Universität Stuttgart
Pfaffenwaldring 6, 70550 Stuttgart, Germany

ABSTRACT

Desorption of hydrogen from metal hydrides requires a supply of reaction enthalpy, absorption requires the removal of this enthalpy. Therefore, the effective thermal conductivity λ_e of the powdered metal hydride strongly influences the velocity of absorbing and desorbing hydrogen.

Based on the cellular-model by Zehner, Bauer and Schlünder (1970, 1972, 1978) for porous media with inert void gases, an extended model is developed to calculate λ_e of powdery materials with a reaction between gas and solid. This reaction causes an elastic expansion of the particles. The extended model also takes into account methods of increasing λ_e such as a built-in metallic matrix.

Experimental investigations have been carried out on the low temperature hydride HWT 5800 ($Ti_{0.98}Zr_{0.02}V_{0.43}Fe_{0.09}Cr_{0.05}Mn_{1.5}H_x$, $x_{max} = 3$) and on the medium temperature hydride $LaNi_{4.7}Al_{0.3}H_x$ ($x_{max} = 6$) within the temperature ranges of $-80 < \vartheta < 20\,°C$ and $-20 < \vartheta < 140\,°C$ respectively and in the pressure range of $10^{-6} < p < 6\,MPa$. The porosity of the pure metal powder is originally 44.5 and 53.1 %. The measurement principle used is the transient hot-wire method.

The paper concludes with a comparison of measured and calculated values of the effective thermal conductivity of different metal hydrides. The design of chemical hydrogen storage devices can thus be based on improved predictions of λ_e.

1   INTRODUCTION

Metal-hydrides have considerable potential for sorption heat pumps, chemical compressors and hydrogen storage. They have fast kinetics and can absorb, and reversibly desorb, large amounts of hydrogen at constant temperature and pressure. Along the pressure plateau only the hydrogen concentration varies (fig. 1). Compared to a gas pressure tank at 20 MPa the hydrogen density is about five times higher. The major difficulties associated with the use of metal hydrides for hydrogen storage are the low maximum hydrogen content of around 2 % by weight, a low thermal conductivity and insufficient reaction kinetic data for many candidate hydrides.

The kinetics of the hydriding process are described in terms of a shrinking core model. The core is taken to be saturated α-phase metal, while hydride is the β-phase. The α-phase is a solid solution of hydrogen in the alloy lattice, the hydrogen interstitials occupy the possible sites randomly. The β-phase is the stoichiometric hydride, the hydrogen may assume a periodic arrangement and thus a long range order. Four steps are involved: chemisorption of H_2 molecules at the surface, dissociation of the H_2 molecules into H atoms, diffusion of H atoms through the hydride and phase change at the hydride interface ($\alpha + H \rightarrow \beta$). This phase change leads to an elastic expansion of the particles while the hydrogen pressure is nearly constant. The resulting additional compression of the particles in a closed container causes a growth of their contact areas and a corresponding growth of λ_e. On the other hand
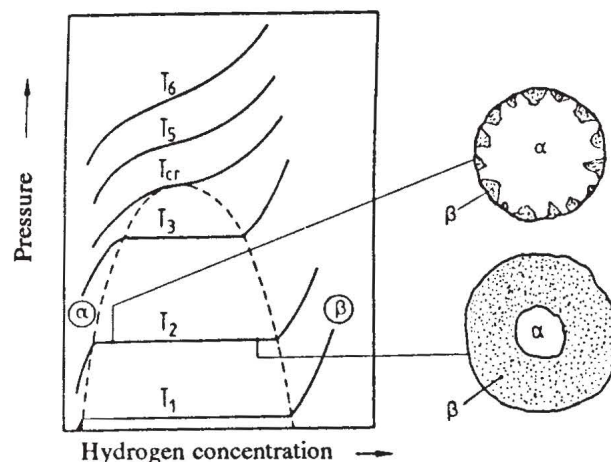

Fig. 1: Pressure-concentration isotherms (P-C-T)

the thermal conductivity of the solid decreases because of the increasing hydrogen concentration disturbing the structure of the crystal lattice.

Results of roughly 15 experimental investigations of the effective thermal conductivity of metal hydrides have been published so far. These references have been listed by Kallweit (1994). A few of the experimental results are given in terms of correlations. A simple theoretical model based on an idea of Masamune and Smith (1963) has been presented by Sun and Deng (1990). Pons and Dantzer (1991) selected the Zehner, Bauer and Schlünder model to study the basic mechanism of thermal conductivity in hydride beds.

2 DETAILS OF THE EXPERIMENTS

The measurement principle of the transient hot-wire method is based on the solution of the transient heat conduction equation. For an ideal continuous line source in an infinite homogeneous and isotropic medium, which - being initially at a uniform temperature T_0 - is suddenly heated by a steady current, we obtain eq. (1) as an approximate solution for large times t (Carslaw and Jaeger, 1959):

$$\Delta T = T(r_w, t) - T_0 = \frac{\dot{q}_L}{4 \pi \lambda_e} \ln \frac{4 \kappa_e t}{r_w^2 C} , \qquad (1)$$

where ΔT is the temperature rise at the surface of the line source (radius r_w), $\dot{q}_L$ is the heat dissipated per unit length of the line source, and $\ln C = 0.5722$ is Euler's Constant, λ_e and κ_e are the effective thermal conductivity and the effective thermal diffusivity of the medium, respectively. If the thermal diffusivity can be considered constant in the small temperature range ΔT ($\Delta T < 2$ K in our measurements), the thermal conductivity can be determined by differentiating ΔT with respect to ln t, such that

$$\lambda_e = \frac{\dot{q}_L}{4 \pi} \left/ \frac{d(\Delta T)}{d(\ln t)} \right. . \qquad (2)$$

The values of $d(\Delta T)/d(\ln t)$ can be read from a diagram of ΔT versus ln t as plotted in a test run.

An electrically isolated (PTFE) platinum wire of 0.2 mm diameter is used as both heat source and resistance thermometer. The platinum wire forms one arm of a high-precision Kelvin bridge; an adjustable resistor with a very low temperature coefficient forms the other arm (fig. 2). The measuring cell, a steel tube of $V_{net} = 217$ cm^3, is contained in a pressure chamber which is designed for pressures from vacuum up to 6.2 MPa and for temperatures up to 370 °C (fig. 3).

Beds of metal hydride powder with porosities of 53.1 % (LaNi$_{4.7}$Al$_{0.3}$) and 44.5 % (HWT 5800) and with medium particle sizes of 36 microns and 250 microns, respectively, have been used as samples. The steel tube contains the metal powder together with the heating wire ($l_w = 117.1$ mm) and its holder. The tube is closed off at both ends with porous steel plates for hydrogen inlet and outlet.
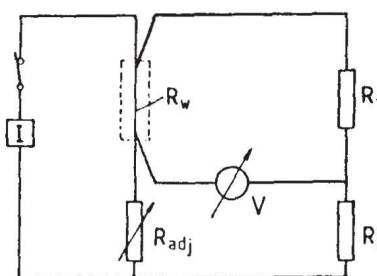

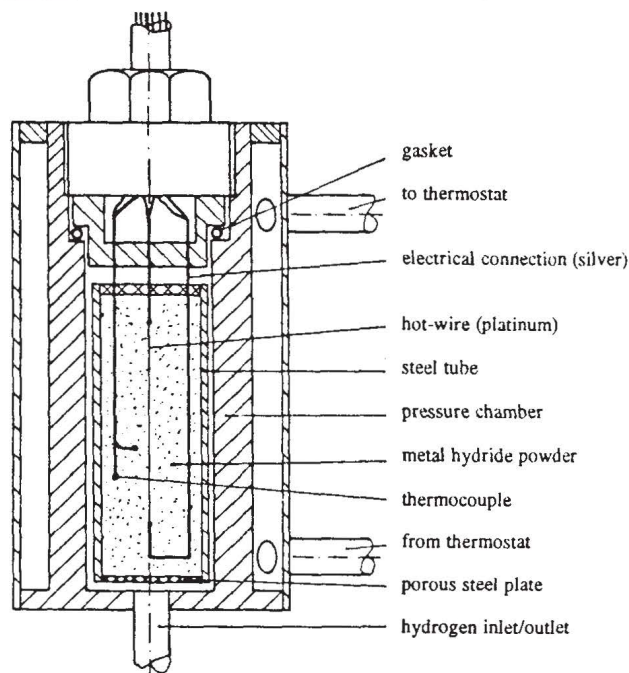Fig. 2: Schematic view of the electric setup

Fig. 3: Schematic view of the test cell

The pressure chamber is temperature controlled. After the activation of the metal powder (by heating up to 200 °C under vacuum conditions) the sample is filled with hydrogen step by step. The measurement process starts when isothermal conditions inside the sample are reached. The two thermocouples controlling this condition are also shown in fig. 3. It is very important to note, that the mean particle size of both materials degrades to less than 10 microns after ten absorption/desorption cycles due to the expansion during interstitial deposition of hydrogen in the metal. Consequently the grain size distribution changes from polydisperse to monodisperse.

3 THEORETICAL MODELLING

3.1 Materials without reaction between gas and solid

The cellular model by Zehner, Bauer and Schlünder (1970, 1972, 1978) for porous media with inert void gases is shown in fig. 4. The unit cell is constructed such that one part of the heat is transferred only through the gas phase of the packing with the relative area $1 - \sqrt{1-\psi}$ by molecular conduction as well as by radiation. The other part passes through both the gas and the solid phase; its relative area is $\sqrt{1-\psi}$, where ψ ($= V_g/V_{total}$) is the porosity of the packing. This separation is necessary in order to describe effective coefficients of diffusion in packings through which there is no flow, which have been obtained empirically.
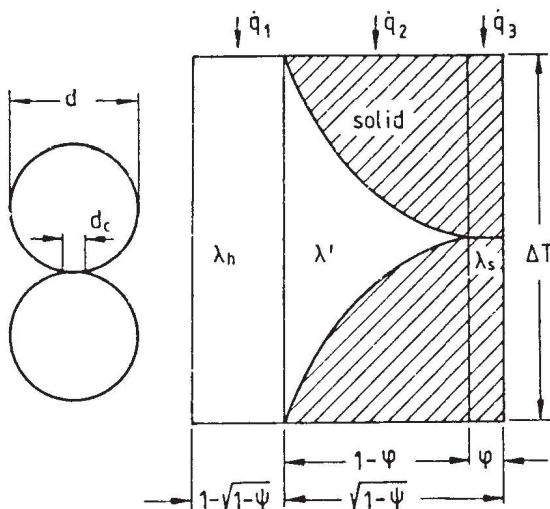

Fig. 4: Schematic view of the unit cell

Contrary to nearly all previously developed models contact between the particles is not understood as point contact. The relative area $\sqrt{1-\psi}$ is therefore further divided by the flattening coefficient φ that describes the additional heat transfer through the solid path between continuous particles. The remaining segment $1-\varphi$ includes heat transfer through the two particle halves which are separated by a wedge of gas. The flattening coefficient φ is correlated to the contact area fraction between two particles ξ_c^2 ($= (d_c/d)^2$):

$$\varphi = \frac{23 \, \xi_c^2}{1 + 22 \, \xi_c^{4/3}} \, , \qquad (3)$$

as given by Bauer and Schlünder (1978).

The effective thermal conductivity of this arrangement can be determined mathematically by the following simplification: the thermal conductivity perpendicular to the direction of heat flow is assumed to be very small and the differential parallel resistances are summed over the surface. To minimize the error caused by this simplification a variable shape of the model particle has been introduced. With the help of the deformation factor B ($= 1.4 \, ((1 - \psi)/\psi)^{10/9})$ the exterior contour of the model particle is modified such that the isothermal lines become flat vertical to the direction of heat flow.

The effective thermal conductivity of the unit cell and consequently of the packing can then be written as eq. (4), assuming mainly parallel connection of the thermal resistances.

$$\lambda_e = (1 - \sqrt{1-\psi}) \, \lambda_h + \sqrt{1-\psi} \, [(1-\varphi) \, \lambda' + \varphi \, \lambda_s] \qquad (4)$$

Both the equivalent conductivity of the hollow space, λ_h, and the equivalent conductivity of the wedge of gas and part of the solid, λ', are functions of the modified Knudsen-number Kn^* and the Nusselt-number Nu_r representing radiation:

$$Kn^* = \frac{2-a}{a} \, \frac{2k}{\gamma+1} \, \tilde{\lambda} \, \frac{2}{d} \qquad (5)$$

$$Nu_r = \frac{4 \, \sigma \, T^3}{(2/\epsilon)-1} \, \frac{d}{\lambda_g} \qquad (6)$$

Here a is the accomodation coefficient, k the ratio $\lambda_g/(\eta_g \, c_v)$ and σ the Stefan-Boltzmann Constant. The equations to calculate λ_h, λ' and the required properties and coefficients for metal powders and for metal hydrides are summarized by Kallweit (1994).

Fig. 5 shows the comparison of experimental and theoretical values of the effective thermal conductivity for two samples (not activated) with inert void gases. The typical S-shapes are represented very well, the conformity between measurement and calculation is good. The transition regime between free molecule- (p $<$ 10^{-5} MPa) and continuum-conditions
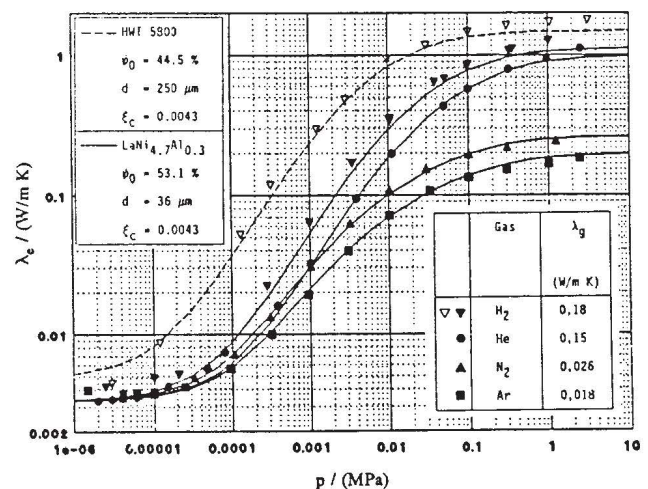

Fig. 5: λ_e of LaNi$_{4.7}$Al$_{0.3}$ and HWT 5800 at $\vartheta = 20$ °C (symbols: measurement, curves: calculation)

375

(p > 0.1 MPa) of the HWT 5800 bulk with hydrogen as a void gas lies at a pressure which is roughly one order of magnitude lower than that of $LaNi_{4.7}Al_{0.3}$. Reason is the lower mean particle size of $LaNi_{4.7}Al_{0.3}$ which is about one tenth of that of HWT 5800 before absorbing and desorbing hydrogen. The lower porosity of HWT 5800 becomes obvious at higher pressures. Here the lower porosity of HWT 5800 leads to a higher λ_e.

3.2 Extended model for metal hydrides

The interstitial deposition of hydrogen in the metal is associated with a phase change and leads to an elastic expansion of the particles. This process changes the porosity, the thermal conductivity of the solid λ_s and above all the contact area fraction.

Experimental investigations by Peisl (1978) showed, that the volume of the metal normally grows by about $\Delta V = 2.9 \times 10^{-30}$ m^3/H-atom. With this value the maximum expansion factor f_{VE} of the particles can be calculated:

$$f_{VE} = \Delta V \, N_A \, x_{max} \, \rho_s \, 2 \times 10^{-3}/(\tilde{M}_s \, \tilde{M}_{H2}) , \qquad (7)$$

where the unit of x_{max} is (g H_2/mol metal) and N_A is Avogadro's constant. For $LaNi_{4.7}Al_{0.3}$ we obtain $f_{VE} = 18.4$ % and for HWT 5800 we find $f_{VE} = 19.7$ %. The relative expansion can be expressed by eq. (8), where $V_{s,0}$ is the volume of the pure metal particle.

$$\frac{\Delta V_s}{V_{s,0}} = f_{VE} \frac{x}{x_{max}} \qquad (8)$$

The absorption of hydrogen in the reactor normally takes place without any deformation of the container. So the expansion of the particles leads to a decrease of the porosity according to:

$$\psi = \psi_0 - (1 - \psi_0) f_{VE} \, x/x_{max} . \qquad (9)$$

Here, too, ψ_0 is the porosity of the metal powder without deposited hydrogen.

Assuming that the thermal conductivity of the solid decreases with increasing hydrogen concentration, we obtain a linear expression for λ_s:

$$\lambda_s = \lambda_{s,0} - (\lambda_{s,0} - \lambda_s^*) \, x/x_{max} . \qquad (10)$$

Here λ_s^* is the thermal conductivity of the β-phase hydride with $\lambda_s^* = (0.7 \div 0.8) \lambda_{s,0}$, according to our measurements. $\lambda_{s,0}$ is the thermal conductivity of the metal particle without deposited hydrogen.

To describe the increasing contact area fraction the following basic idea is used: In the reactor two limiting cases for the expanding particles are conceivable: The lower limit is a constant contact area fraction during the expansion (ξ_c = const.), the upper limit results from assuming the particles to be fully restrained between two plates ($\xi_c > \xi_{c,0}$) as shown in fig. 6. In reality the change of the contact area fraction lies somewhere between these two limitations.
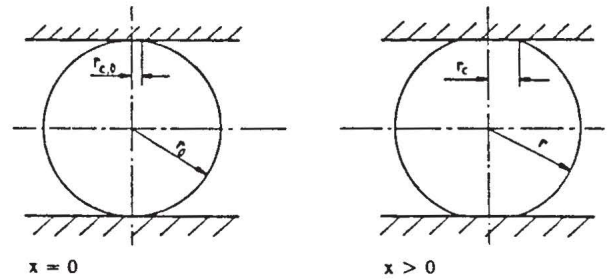

Fig. 6: Fully restrained particle during expansion

If the contact area fraction at the beginning is known ($0.004 < \xi_{c,0} < 0.008$), the flattened radius $r_{c,0}$ can be used to calculate the force between two particles with the help of Hertz's first formula:

$$F_0 = r_{c,0}^3 \, \frac{4}{3} \, \frac{E}{1 - \mu^2} \, \frac{1}{r_0} . \qquad (11)$$

E is Young's modulus and μ the transverse contraction ratio (Poisson's ratio). Hertz's second formula describes the way in which the centres of two spheres approach each other if they are subjected to a known force F_x. After rearranging appropriately one can also calculate the force F_x resulting from the expansion of a particle fully restrained between two plates:

$$F_x = \sqrt{\frac{16 \left[\frac{f_{VE}}{3} \frac{x}{x_{max}} \right]^3 E^2 \, r_0^4}{9 \, (1 - \mu^2)^2}} . \qquad (12)$$

Now both limiting cases are combined into the "force factor" f_F:

$$F = F_0 + f_F \, F_x . \qquad (13)$$

The force factor reduces the fictitious full restrainment of the particles to their realistic mutual interference in the reactor. $f_F = 0$ corresponds to free expansion of the particles while $f_F = 1$ represents full restrainment. By using the force F which depends on the hydrogen concentration (x in eq. (12)), the growth of contact area fraction can be estimated. Based on our own measurements and measurements reported by other authors we have succeeded to estimate f_F, if the

376

porosity of pure metal powder, ψ_0, and the maximum expansion of the material, f_{VE}, are known:

$$f_F = \psi_0 (0.55 - 0.035 \, f_{VE}) + 2.285 \, f_{VE} - 35.8 \quad (14)$$

with: $f_{VE} > 15.5 \%$ and $40 \% < \psi_0 < 60 \%$.

Usually the force factor f_F lies between 0 and 4 %. Now the actual force F, eq. (13), the flattened radius r_c, eq. (11), the contact area fraction ξ_c and the flattening coefficient φ, eq. (3), become calculable. With the porosity ψ, eq. (9), and the thermal conductivity of the solid λ_s, eq. (10), both also depending on the hydrogen concentration, the effective thermal conductivity of the hydride is given by eq. (4).

Figures 7 and 8 show plots of experimental (symbols) and theoretical values (curves) of the effective thermal conductivity of LaNi$_{4.7}$Al$_{0.3}$H$_x$ and HWT 5800 versus hydrogen pressure. The S-shape is now modified due to the expansion of the particles in the region of the temperature dependent plateau of pressure (comp. fig. 1). The equations to estimate the equilibrium pressure depending on temperature and hydrogen concentration are given by Nishizaki et al. (1983).
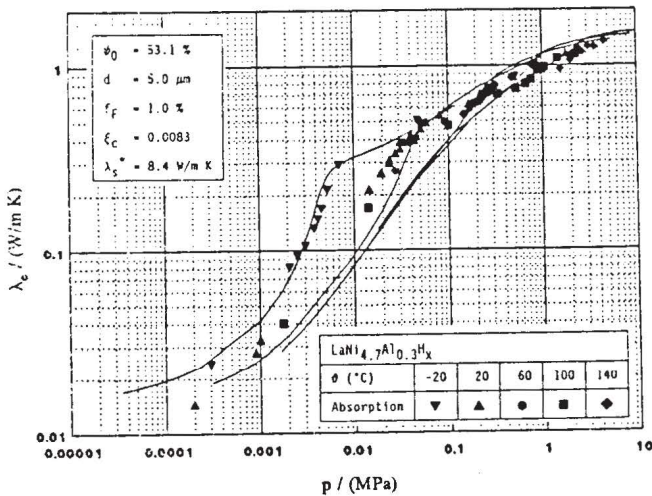

Fig. 7: λ_e of LaNi$_{4.7}$Al$_{0.3}$H$_x$ ($\vartheta = -20 \div 140 \,°C$)

The experiments were conducted after more than 10 absorption and desorption cyles, so that the mean particle size was less than 10 microns. A further decrease of the mean particle size is insignificant for λ_e. In fig. 8 it is seen, that at low pressures λ_e is much higher than at the starting conditions shown in fig. 5. The increase results from the change of the particle size distribution from polydisperse to monodisperse. With a monodisperse distribution the bed would normally have a larger porosity. Since the steel tube volume remains the same the porosity cannot change and the forces between the particles increase accordingly.

The force factor describing the expansion of the particles is $f_F = 1 \%$ for LaNi$_{4.7}$Al$_{0.3}$H$_x$ and 3 % for HWT 5800 as obtained from eq. (14).
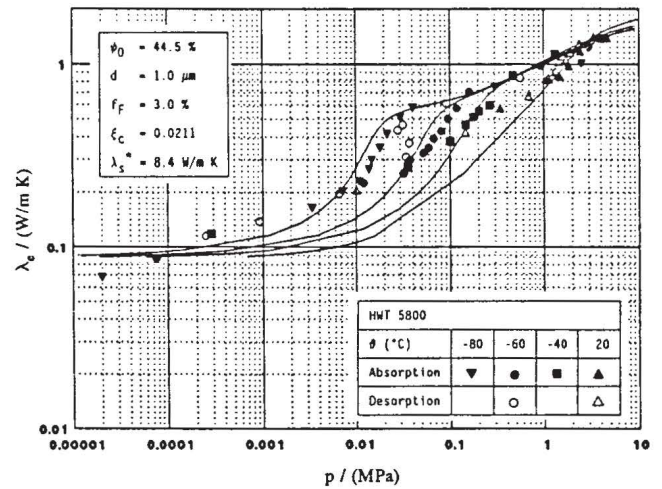

Fig. 8: λ_e of HWT 5800 ($\vartheta = -80 \div 20 \,°C$)

3.3 Extended model with built-in metallic matrix

Two kinds of metallic matrix are commonly considered for the increase of the poor effective thermal conductivity of metal hydride powders:

- three-dimensional structures of porous aluminium or nickel composite (metallic foam);
- multiple waved sheet metal structures.

The model for the metallic foam is shown in fig. 9. By means of the electrical-analogy the effective thermal conductivity of such a powder-matrix composite $\lambda_{e,m}$ can be estimated. The input parameters are the porosity of the matrix ψ_m, the thermal conductivity of the matrix λ_m and the effective thermal conductivity of the powder λ_e. The heat transfer coefficient between matrix and powder α_m takes on values above 500 W/m^2 K. Its influence on $\lambda_{e,m}$ is negligible.
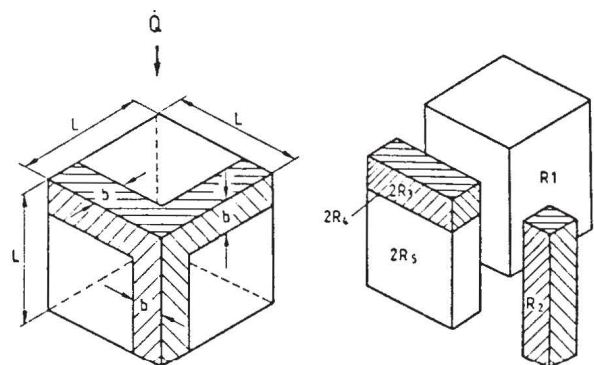

Fig. 9: Model for the metallic foam

The equivalent circuit diagram for the metallic foam matrix is shown in fig. 10. The resistances are listed.

$$R_1 = L/[\lambda_e (L-b)^2]$$

$$R_2 = L/[\lambda_m b^2]$$

$$R_3 = b/[2 \lambda_m b (L-b)]$$

$$R_4 = [2 \alpha_m b (L-b)]^{-1}$$
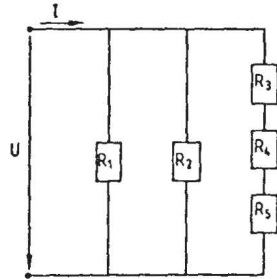
$$R_5 = (L-b)/[2 \lambda_e b (L-b)]$$

Fig. 10: Equivalent circuit

The width b of the paths is given by the porosity of the matrix ψ_m:

$$(1 - \psi_m) L^3 = 2 b^2 (L - b) + b^2 L \qquad (15)$$

The overall resistance R_{ov} can be determined with the rules of serial and parallel connection of resistances:

$$R_{ov} = \frac{R_1 R_2 (R_3 + R_4 + R_5)}{R_1(R_2 + R_3 + R_4 + R_5) + R_2(R_3 + R_4 + R_5)} \qquad (16)$$

The thermal conductivity of the composite is then given by:

$$\lambda_{e,m} = (L\, R_{ov})^{-1} \ , \qquad (17)$$

where the length L of the paths is arbitrary.

A final comparison between theoretical values of $\lambda_{e,m}$ of $MmNi_{4.5}Al_{0.5}H_x$ with aluminium and nickel foam, respectively, and measurements by Suda et al. (1983) is shown in fig. 11. The porosities of the
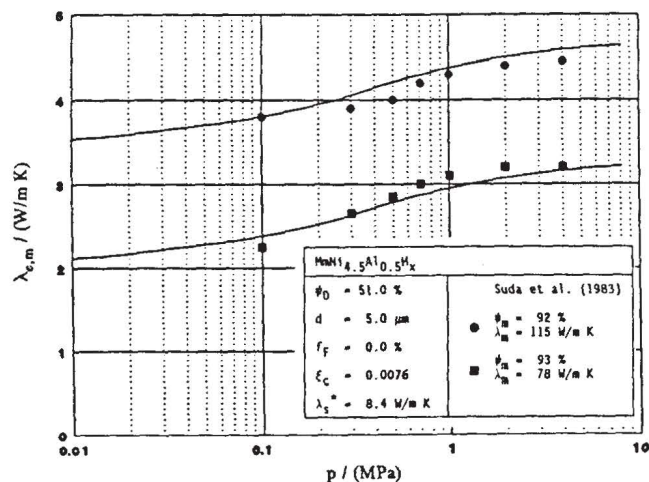

Fig. 11: $\lambda_{e,m}$ of composite material ($\vartheta = 35\ °C$)

matrices are 92 % and 93 %, respectively, the thermal conductivities are 115 W/m K and 78 W/m K, respectively. The force factor f_F here is 0 % because of the low maximum expansion f_{VE} of approximately 15.5 %. Therefore no additional effect in the plateau of pressure can be recognized. The effective thermal conductivity now shows values that are roughly three to four times higher than the effective thermal conductivity of the powder alone.

ACKNOWLEDGEMENT

REFERENCES

Bauer, R. & Schlünder, E. U. (1978), Effective radial thermal conductivity of packings in gas flow. Part II: Thermal conductivity of the packing fraction without gas flow, Int. Chem. Eng., vol. 18, no. 2, pp. 189-204.

Carslaw, H. S. & Jaeger, J. C. (1959), Conduction of heat in solids, second edition, Oxford University Press, p. 117, p. 261, pp. 342-345.

Kallweit, J. (1994), Effektive Wärmeleitfähigkeit von Metallhydrid-Materialien zur Speicherung von Wasserstoff, Ph.D. thesis, Universität Stuttgart.

Masamune, S. & Smith, J. M. (1963), Thermal conductivity of beds of spherical particles, Ind. Eng. Chem. Fundam., vol. 2, no. 2, pp. 136-143.

Nishizaki, T., Miyamoto, K. & Yoshida, K. (1983), Coefficients of performance of hydride heat pumps, J. Less-Common Metals, vol. 89, pp. 559-566.

Peisl, H. (1978), Wasserstoff in Metallen, Physik in unserer Zeit, vol. 9, no. 2, pp. 37-45.

Pons, M. & Dantzer, P. (1991), Effective thermal conductivity in hydride packed beds. I. Study of basic mechanism with help of the Bauer and Schlünder model, J. Less-Common Metals, vol. 172-174, pp. 1147-1156.

Suda, S., Komazaki, Y. & Kobayashi, N. (1983), Effective thermal conductivity of metal hydride beds, J. Less-Common Metals, vol. 89, pp. 317-324.

Sun, D. W. & Deng, S. J. (1990), A theoretical model predicting the effective thermal conductivity in powdered metal hydride beds, Int. J. Hydrogen Energy, vol. 15, no. 5, pp. 331-336.

Zehner, P. & Schlünder, E. U. (1970), Wärmeleitfähigkeit von Schüttungen bei mäßigen Temperaturen, Chem.-Ing.-Techn., vol. 42, no. 14, pp. 933-941.

Zehner, P. & Schlünder, E. U. (1972), Einfluß der Wärmestrahlung und des Druckes auf den Wärmetransport in nicht durchströmten Schüttungen, Chem.-Ing.-Techn., vol. 44, no. 23, pp. 1303-1308.